JOURNAL OF MATERIALS SCIENCE 14 (1979) 2713–2720

A fractographic criterion for subcritical crack growth boundaries at internal fracture origins in hot pressed silicon nitride

H. P. KIRCHNER, R. M. GRUVER, D. M. RICHARD
Ceramic Finishing Company, P.O. Box 498, State College, PA 16801, USA

Using the elliptic integral method, stress intensity factors (K_I) were estimated at boundaries defined by fracture features observed at various distances from internal fracture origins in H.P. silicon nitride. The fracture origins are surrounded by regions of transgranular fracture. At the outer boundaries of these regions K_I is less than K_{IC} showing that these are regions of subcritical crack growth. Regions of hummocks and depressions were observed surrounding the regions of transgranular fracture. K_I was calculated at the elliptical boundary determined by the outer edge of the nearest of these features to the fracture origin. At this boundary, $K_I \approx K_{IC}$. Therefore, these features can be used to locate the subcritical crack growth boundary.

1. Introduction

Development of fracture theories and methods of failure analysis has been handicapped by the lack of fractographic criteria for locating subcritical crack growth boundaries in fracture surfaces of ceramics. In this paper such a criterion is described for a particular hot pressed (H.P.) silicon nitride ceramic.

Fracture origins in H.P. silicon nitride, fractured at room temperature, are easily located in most cases at the intersection of the extensions of lines drawn through the hackle. In some cases other types of lines oriented in the direction of the fracture origin can be observed in the fracture surface. Because the material is strong and fine grained, these fracture features are well defined, aiding in location of the fracture origins. Although individual grains in fracture surfaces may strongly reflect incident light, the areas of reflecting spots that are so helpful in locating fracture origins in alumina ceramics are not observed in H.P. silicon nitride.

Flaws at fracture origins in H.P. silicon nitride specimens, fractured at various temperatures and loading rates, were located and characterized by Kirchner, Gruver and Sotter [1, 2] and Baratta, Driscoll and Katz [3]. Recently, D. G. Miller *et al.* [4] described a number of such flaws. At room temperature, fracture may originate at various types of flaws including machining damage, pores, large crystals and inclusions. However, with improved surface finish and increased volume under stress (tensile tests or large specimens) there is increased tendency for fracture to originate at internal flaws, frequently inclusions associated with pores. The fracture stress increases with increasing transformation of alpha to beta silicon nitride [5, 6]. This increase has been attributed to increased particle elongation.

Attempts to measure the variation of crack velocity with stress intensity factor (K_I) at room temperature using standard techniques such as the double torsion beam test have, thus far, not been successful. Apparently, crack velocity increases so rapidly with K_I that it has not been possible to achieve stable crack propagation. However, there is a small slow crack growth effect in H.P. silicon nitride [1]. Twenty cylindrical rods were loaded in flexure to a constant stress of 629 MPa in air at 18 to 22% relative humidity. Four of the specimens fractured on loading (< 1 sec) and seven survived for more than 1000 sec after which the test was terminated. The remaining specimens (nine) fractured after various times

0022–2461/79/112713–08 $02.80/0

ranging from one to 863 sec. Results consistent with these observations were obtained by Gulden and Metcalfe [7]. They observed a substantial stress corrosion effect but 10% of the fractures originated at internal flaws to which the test environment did not have direct access perhaps showing that a corrosive environment is not necessary for slow crack growth to occur in this material.

Evans and Tappin [8] and Bansal, Duckworth and Niesz [9, 10] have attempted to locate critical flaw boundaries after subcritical crack growth and flaw linking in several ceramics. However, as indicated by Rice [11], considerable subjective judgement is involved in such attempts. It would be desirable to have more objective criteria for locating these boundaries. Kirchner and Gruver [12, 13] have used the variation of the per cent intergranular fracture (PIF) with K_I to develop such criteria for H.P. alumina and 96% alumina. In the present investigation, this technique was used to develop a criterion for locating subcritical crack growth boundaries in silicon nitride.

2. Procedures

The present research was done by fractographic analysis of H.P. silicon nitride specimens* fractured in tension in an earlier investigation. Preparation and testing of these specimens was described previously [1. 7]. The specimens were cylindrical rods necked down to form a test section about 1.4 mm diameter. The loading rate was rather slow, requiring more than one minute to fracture the specimens. The fracture surfaces were studied by optical and scanning electron microscopy (SEM) including stereo SEM.

The fractures originated at internal flaws which were surrounded by regions of transgranular fracture. Two principal methods of analysis were used. The first method involved outlining the outer boundary of the region of transgranular fracture and using the elliptic integral method [14] to calculate the stress intensity factors at the intersections of the major and minor axes with this boundary. The stress intensity factor (K_I) was calculated using

$$K_I = \frac{Y\sigma}{\Phi}\left(\frac{a}{c}\right)^{1/2}(a^2\cos^2\theta + c^2\sin^2\theta)^{1/4} \quad (1)$$

in which a, c and θ are defined as in Fig. 1. That is, a is $\frac{1}{2}$ the minor axis of the ellipse, c is $\frac{1}{2}$ the major axis of the ellipse, and θ is the angle between the major axis and a radius of the ellipse. Φ is defined by the following integral

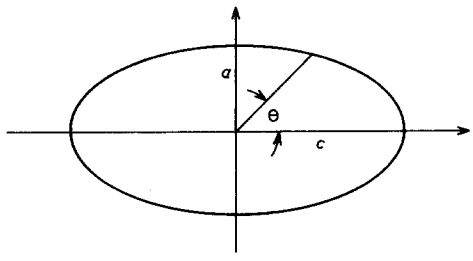

Figure 1 Definition of a, c and θ.

$$\Phi = \int_0^{\pi/2}\left[1 - \left(1 - \frac{a^2}{c^2}\right)\sin^2\theta\right]^{1/2} d\theta \quad (2)$$

which is an elliptic integral of the second kind. Mathematical tables were used to determine the values of this integral. To determine K_I at the intersection of the minor axes with the boundary of the ellipse, θ is taken as $\pi/2$ in Equation 1 yielding

$$K_{I_{max}}\left(\theta = \frac{\pi}{2}\right) = \frac{Y\sigma}{\Phi}a^{1/2} \quad (3)$$

Similarly, for the intersection with the major axis

$$K_{I_{min}}(\theta = 0) = \frac{Y\sigma}{\Phi}a^{1/2}\left(\frac{a}{c}\right)^{1/2} \quad (4)$$

The values of K_I were compared with the critical stress intensity factor (K_{IC}).

The second method involved determining the percentages of intergranular and transgranular fracture along radii from the fracture origin. Scanning electron micrographs (1000 to 5000 ×) were taken at intervals along the radii and assembled to form composite photographs of the fracture surfaces. A grid with spaces approximately equal to one grain size and ten spaces wide was prepared. The grid was placed on the composite photograph and the fracture surface at the centre of each grid space was examined and classified as to whether it was intergranular or transgranular, characterizing a path about ten grains wide. This process was repeated for adjoining rows of the grid. The percentages of intergranular and

*NC-132, Norton Company, Worcester, MA, USA.

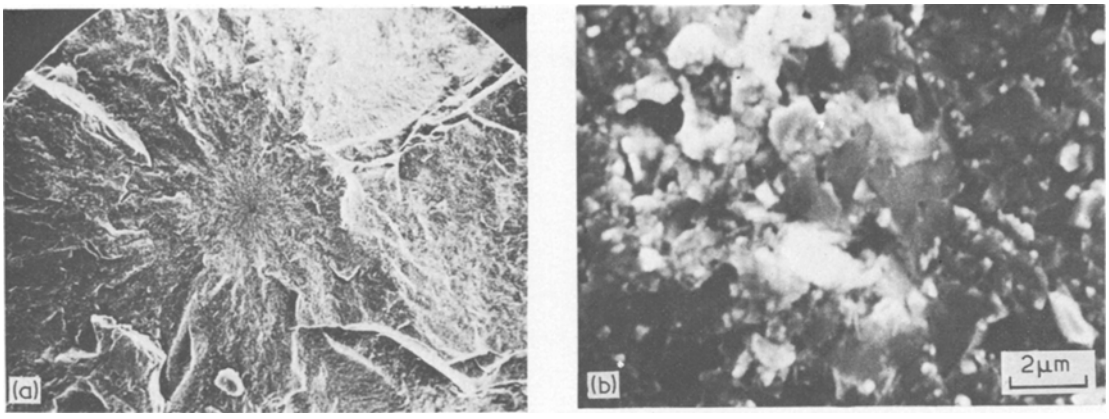

Figure 2 Fracture surface and internal fracture origin, specimen 2T. (a) fracture surface (× 50); (b) fracture origin (× 4900).

transgranular fracture varied considerably from one row to the next so averages were calculated for each row which included the results of the preceding and following rows to form three row running averages. The percentages of intergranular fracture (PIF) were plotted versus the stress intensity factors calculated at the various points along the radii when the crack front was at each point. The calculations of K_I were done using the fracture stress so that the results are strictly correct only for delayed fracture (constant load) specimens for which the applied stress is constant. For specimens fractured by a linearly increasing load, the K_I values are overestimated at all crack lengths except the critical crack length because the stress is overestimated. However, calculations show that almost all of the crack growth occurs in less than the last 10% of the loading time. In this time the applied stress varies by less than 10%. Therefore, the error in the calculated K_I values is small for most of the crack growth.

3. Results and discussion

3.1. General observations

Most of the results of this investigation were obtained from five specimens fractured in uniform tension. All of the fractures originated at what appeared to be inclusions, pores or porous regions (Fig. 2). The flaws at the fracture origins ranged in size from the average grain size (1 to 2 μm) to several times that size. When the fracture surfaces were rotated in the SEM, it was observed that, in particular orientations, each fracture origin was surrounded by a rather dark elliptical region (Fig. 3). Such a dark region was observed previously by Baratta *et al.* [3] At slightly higher magnification it was observed that these regions contained a large fraction of transgranularly fractured grains (Fig. 4).

Outside the dark elliptical region is a region in which the surface is more uneven, as indicated by light and dark blotches. At higher magnification using stereo SEM these blotches are ob-

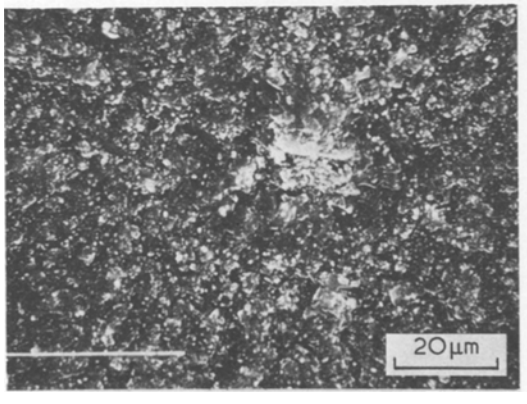

Figure 3 Dark region surrounding fracture origin, specimen 4T (× 680).

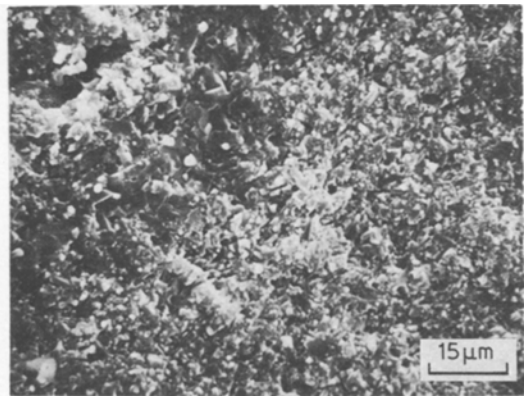

Figure 4 Transgranular fracture at fracture origin, specimen 1T (× 3400).

TABLE I Stress intensity factors* at the boundaries of the dark ellipses in H.P. Si_3N_4 specimens fractured in tension

Specimen number	Fracture stress (MPa)	Minor axis (a) (μm)	Major axis (c) (μm)	Eccentricity (a/c)	Φ	Stress intensity factor	
						$K_{I_{max}}$ (MPa $m^{1/2}$)	$K_{I_{min}}$ (MPa $m^{1/2}$)
1T	529	17	31	.55	1.242	3.16	2.34
2T	896	9	11	.82	1.432	3.38	3.06
3T	716	20	36.7	.54	1.240	4.65	3.42
4T	651	19	23	.83	1.437	3.55	3.23
5T	708	17.5	35	.50	1.211	4.40	3.11

*$K_{I_{max}} = \frac{Y\sigma_f(a)^{1/2}}{\Phi}$ where Y was taken as 1.8 for internal flaws.

served to be hummocks and depressions which form a wide band outside the dark elliptical region.

Numerous pores are observed in the wide band of hummocks and depressions. Many of these pores are surrounded by small regions of transgranular fracture. These observations are additional evidence of the tendency of cracks originating at pores to grow by subcritical crack growth.

3.2. Stress intensity factors at boundaries of dark elliptical regions

The elliptic integral method was used to calculate values of K_I at the intersections of the major and minor axes with the boundaries of these ellipses yielding the results shown in Table I. As expected, the higher values of K_I occur at the intersections of the minor axes with the boundaries of the ellipses. These values range from 3.16 to 4.65 MPa $m^{1/2}$. The highest value is slightly less than a widely accepted value of K_{IC} which is 4.7 MPa $m^{1/2}$ [15, 16].

The K_I values in Table I seem to be too low to support the hypothesis that the subcritical crack growth boundary is the boundary of the dark region of grains fractured mainly by transgranular fracture. Therefore, the fracture surfaces were examined for other features that might serve to locate the subcritical crack growth boundary. Outside the boundary of the dark area are numerous features that might be described as hummocks and depressions as shown in the stereo pairs in Fig. 5 and 6. Many of the hummocks and depressions are elongated radially from the fracture origin. These features are not hackle which are observed at much greater distances from the fracture origin. At low magnification the elongated hummocks and depressions give the fracture surface a somewhat fibrous appearance. The normal range of sizes of these features is about 4 to 8 μm.

Based on the above observations, it was hypothesized that the hummocks consisted of agglomerates that were resistant to fracture so

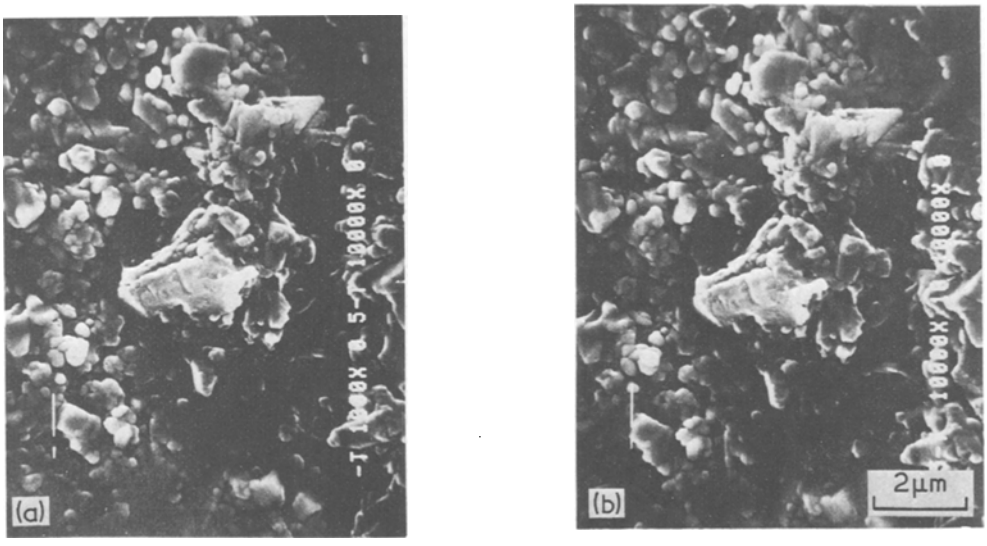

Figure 5 Hummock surrounded by depressions, specimen 5T, stereo pair (× 6000).

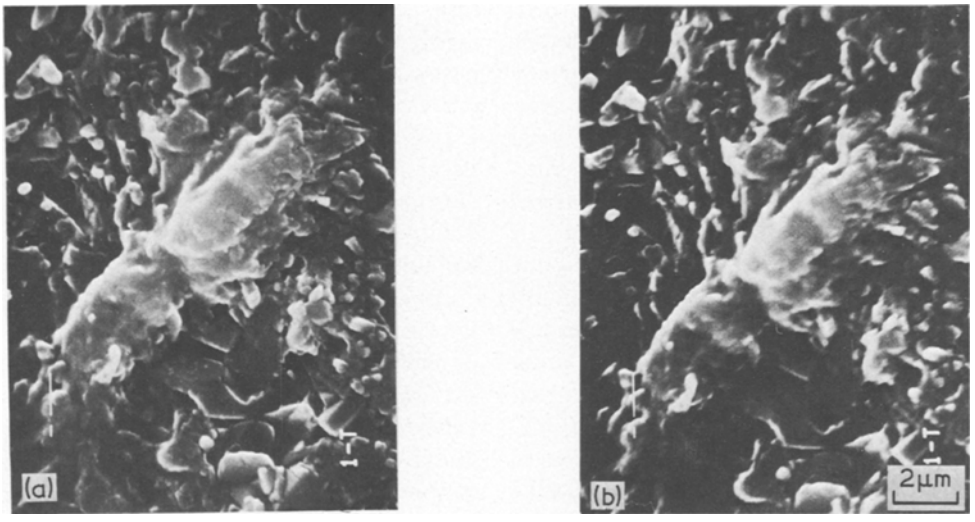

Figure 6 Hummock surrounded by depressions, specimen 1T, stereo pair (× 5800).

that, for crack propagation to occur at the velocity characteristic of the particular K_I value, it is necessary for the crack to propagate around the agglomerates. Assuming this to be the case a rough boundary outside the first "row" of these hummocks and depressions was visualized and the minor axis was measured. The eccentricity of the ellipse was assumed to be the same as that of the dark region. The resulting K_I values are given in Table II. These values are more consistent with the measured K_{IC}.

The fact that these K_I values are somewhat scattered is not surprising because of experimental uncertainties in measurement of the ellipses and local variations in material properties such as K_{IC}. One expects fractures to originate in the regions that have the most vulnerable combination of flaw severity and reduced local K_{IC}.

The mechanism by which the agglomerates resist fracture was studied. An etched fracture photographed by Miller *et al.* [4] shows hummocks and depressions of the same size as those observed in the present investigation. The hummocks appear to contain elongated grains with preferred orientations tending to be perpendicular to the fracture surface. Therefore, the agglomerates may resist fracture because they consist of elongated grains with preferred orientations perpendicular to the crack front. The hummock illustrated in Fig. 6 evidently resisted fracture because of the presence of the elongated grains at the "leading" edge of the hummock. In other cases such as Fig. 6 similar

TABLE II Revised stress intensity factors for boundaries at the far side of hummocks and depressions near minor axis of the dark ellipse

Specimen number	Fracture stress (MPa)	Revised minor axis (a) (μm)	Φ	Revised $K_{I_{max}}$ (MPa m$^{1/2}$)	Revised $K_{I_{min}}$ (MPa m$^{1/2}$)	Comments
1T	529	34	1.242	4.47	3.31	
2T	896	20	1.432	5.04	4.56	
3T	716	20	1.240	4.65	3.42	(a) was not revised because projecting agglomerates were not prominent features
4T	651	30	1.437	4.47	4.07	
5T	708	26	1.211	5.37	3.80	Projecting agglomerates off minor axis
			Average	4.8	3.8	

grains were not observed but may have been present within the hummock. Fig. 28 of Bowen [6], Fig. 6, and some of the composite photographs not included because they are too large, show that the depressions contain many grains elongated parallel to the fracture surface. Interspersed among these grains are individual elongated grains that have either pulled out of the opposite surface of the crack or fractured through the grain. These observations are interpreted to mean that the crack propagates by transgranular fracture until it speeds up to the point that it no longer can pass through the hummocks by transgranular fracture. Therefore, the cracks are deflected over, under and around the hummocks. The preferred paths are those in which the grains are elongated parallel to the fracture surface. In these paths, those grains oriented perpendicular to the fracture surface pull out or fracture, as suggested by Bowen [5, 6], contributing to the fracture resistance.

The ellipticity of the dark regions remains to be explained. The tensile specimens were six in. long and were cut from hot pressed billets, 6 in. x 6 in. x 1 in. The fracture surfaces were roughly perpendicular to the long axes of the specimens so that each surface can be considered to contain axes perpendicular and parallel to the hot pressing direction. It is well known that the average strengths of specimens cut with the long axes parallel to the hot pressing direction are lower than those of specimens cut perpendicular to the hot pressing direction [17]. Therefore, one possible explanation is that the ellipticity is caused by differences in the fracture energies for crack propagation in the directions perpendicular and parallel to the hot pressing direction.

An alternative explanation of the ellipticity of the dark areas is that the flaws are elongated and that the cracks tend to propagate in all directions from the flaw preserving this elongation. Examination of the flaws revealed that they were rather irregular in shape and were more or less elongated. In some cases the ellipticity of the dark region seemed to correspond to that of the flaw. However, it should be noted that the flaws may be elongated perpendicular to the hot pressing direction so that the suggested explanations may not be independent of each other.

The large variations in eccentricity (a/c) of the dark region indicate the possibility of rather large variations in the fracture energy anisotropy and the flaw anisotropy from specimen to specimen. Therefore, the present evidence is most useful for defining the nature of the problem but is not sufficient to permit conclusions to be drawn. In any case, Lange [14] and Miller *et al.* [3] both observed a 20% reduction in the strengths of specimens fractured in the weak direction compared with the strong direction. The average difference between $K_{I_{max}}$ and $K_{I_{min}}$ is consistent with this difference in the strengths.

It is also interesting to note that the fracture mirror (crack branching) boundaries are circular or almost circular indicating that the ellipticity in the early stages of crack propagation does not extend to the later stages. This observation, together with the variations in the mode of fracture, indicates that the mechanism of fracture at branching is not necessarily the same as that near the fracture origin. This has implications for the relative sizes of critical flaws and fracture mirrors in various ceramics.

3.3. Stress intensity factor versus per cent intergranular fracture

The PIF was determined along the major and minor axes of the ellipses formed by the boundaries of the dark areas. The results were somewhat variable, in part because of variations in the quality of the photographs. Emphasis was placed on determinations along the minor axes because the highest K_I values are observed there.

Two of the resulting curves of K_I versus PIF are given in Figs. 7 and 8. At low values of K_I, the PIF is determined mainly by the characteristics of the particular flaw at the fracture origin which may vary widely as indicated in these figures. However, in both cases the curves pass through low values of PIF (high percentages of transgranular fracture) which are followed by a strong trend toward higher PIF.

These curves confirm that the fracture origins are surrounded by a band of primarily transgranular fracture. In addition, they indicate that $K_I = K_{IC}$ in a region of relatively high PIF. This result is consistent with expectations if crack propagation is inhibited by agglomerates that finally pull out when $K_I = K_{IC}$.

Recent data of Govilla [18] raises some doubt about the correctness of the K_{IC} values chosen for use in analysing the above data. Govilla tested nominally similar material and observed $K_{IC} = 4.1\ \text{MPa m}^{1/2}$ (range 3.9 to $4.4\ \text{MPa m}^{1/2}$). Analysis on the basis of Govilla's data would lead

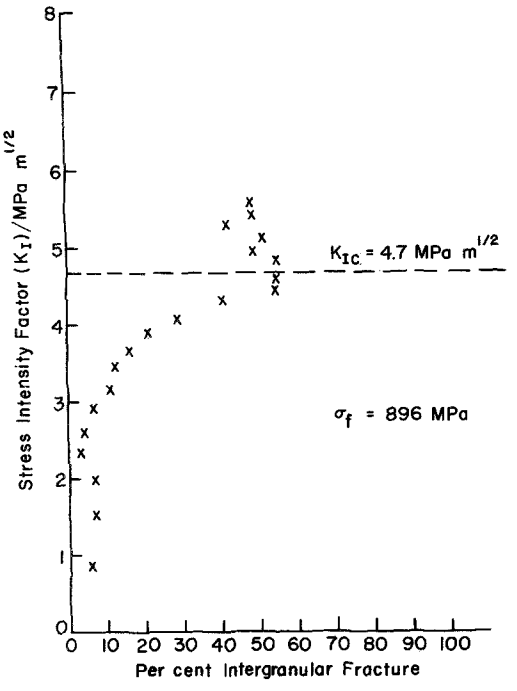

Figure 7 Stress intensity factor versus per cent intergranular fracture, specimen 2*a*T, minor axis of ellipse.

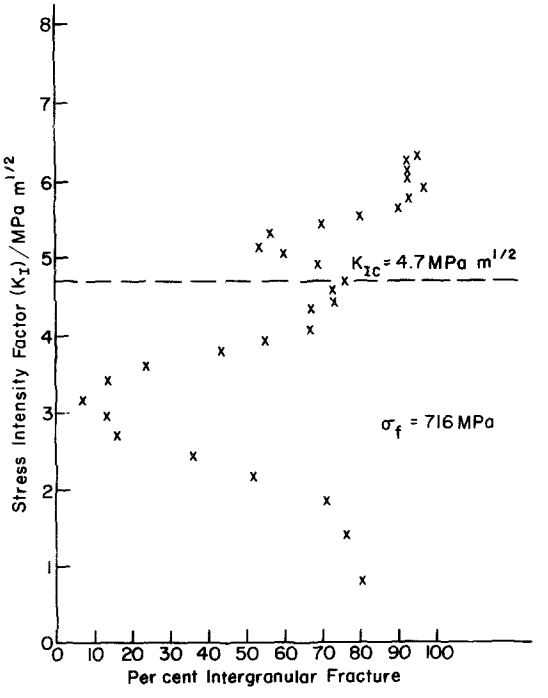

Figure 8 Stress intensity factor versus per cent intergranular fracture, specimen 3T, minor axis of ellipse.

to some difference in interpretation because the subcritical crack growth boundary would be shifted closer to the outer edge of the dark elliptical region. However, the PIF at 4.1 MPa $m^{1/2}$, as indicated in Figs. 7 and 8, is well above the value at minimum PIF so that the difference in fracture modes of H.P. silicon nitride and H.P. alumina at criticality is still evident. Despite the availability of the new data it was decided to retain the original interpretation for the following reasons:

(1) Govilla stressed that his new data are preliminary; (2) the material used in our investigation was manufactured at a much earlier time (1973) and therefore is more likely to be like the materials used by Petrovic *et al.* [16] and Evans and Wiederhorn than that of Govilla; (3) K_{IC} values of Lange [19] for research specimens having varying percentages of α-Si_3N_4 in the starting powders and, therefore, varying degrees of particle elongation, ranged from 4.16 to 6.0 MPa $m^{1/2}$ so that, considering the fact that NC-132 silicon nitride contains a substantial fraction of elongated grains, it seems unlikely that the NC-132 silicon nitride would have K_{IC} as low as 4.1 MPa $m^{1/2}$; and (4) the essential aspects of the interpretation, especially the difference in the fracture mode at the subcritical crack growth boundary compared with that in H.P. alumina, would remain unchanged.

4. Conclusions

Study of fracture origins, dark ellipses surrounding the fracture origins and the hummocks and depressions has shown that there is an orderly sequence of fracture features observed along radii extending from internal fracture origins in H.P. Si_3N_4. Initially, the cracks grow from the fracture origin by transgranular fracture. Similar results were obtained previously for H.P. alumina and 96% alumina [12, 13]. Apparently, as the crack accelerates with increasing K_I, there is insufficient time for transgranular fracture to occur and the crack is forced to find another path. Based on our previous observations in alumina ceramics we would have expected simply increased intergranular fracture. However, this appears to be prevented with the result that the crack diverges from the average fracture plane forming a continuing series of hummocks and depressions. Present evidence indicates that these features are formed because of the presence of fracture resistant agglomerates. This fracture resistance may arise because of the presence of elongated crystals which may tend to bind the agglomerates together. Such an expla-

nation is consistent with the increased strength of H.P. Si_3N_4 bodies derived from high alpha powders which form elongated crystals on conversion to beta silicon nitride [5, 6].

Based on these observations a criterion for locating the subcritical crack growth boundary in a particular silicon nitride, can be suggested. First, the dark elliptical region formed by transgranular fracture should be outlined. Then, the hummocks formed along the extensions of the minor axis of the ellipse should be located. An ellipse of the same eccentricity as the dark region, drawn through the outer edge of the first of these hummocks should coincide approximately with the subcritical crack growth boundary.

Acknowledgements

The writers are pleased to acknowledge helpful discussions with Dr L. J. Bowen of The Pennsylvania State University and the sponsorship of the Naval Air Systems Command.

References

1. R. M. GRUVER, W. A. SOTTER and H. P. KIRCHNER, "Fractography of Ceramics," Ceramic Finishing Company Summary Report, Contract N00019-73-C-0356 (1974).
2. H. P. KIRCHNER, R. M. GRUVER and W. A. SOTTER, *Mater. Sci. Eng.* **22** (1976) 147.
3. F. I. BARATTA, G. W. DRISCOLL and R. N. KATZ, "Ceramics for High Performance Applications, edited by J. J. Burke, A. E. Gorum and R. N. Katz, (Brook Hill Publishing Co, Chestnut Hill, MA 1974), p. 445.
4. D. G. MILLER, C. A. ANDERSSON, S. C. SINGAL, F. F. LANGE, E. S. DIAZ, R. KOSSOWSKY and R. J. BRATTON, "Brittle Materials Design, High Temperature Gas Turbine Material Technology," Vol. IV, Westinghouse Electric Corp. Final Report, AMMRC CTR 76-32, Contract DAAG 46-71-C-0162, (1976).
5. L. J. BOWEN and T. G. CARRUTHERS, *J. Mater. Sci.* **13** (1978) 684.
6. L. J. BOWEN, Ph.D. Thesis, University of Leeds (1977).
7. M. E. GULDEN and A. G. METCALFE, *J. Amer. Ceram. Soc.* **59** (1976) 391.
8. A. G. EVANS and G. TAPPIN, *Proc. Brit. Ceram. Soc.* **20** (1972) 275.
9. G. K. BANSAL, W. H. DUCKWORTH and D. W. NIESZ, *J. Amer. Ceram. Soc.* **59** (1976) 472.
10. G. K. BANSAL and W. H. DUCKWORTH, *ibid.* **60** (1977) 304.
11. R. W. Rice, *ibid.* **61** (1978) 466.
12. H. P. KIRCHNER and R. M. GRUVER, *J. Mater. Sci.* **14** (1979) 3903.
13. H. P. KIRCHNER and R. M. GRUVER, submitted for publication.
14. G. K. BANSAL, *J. Amer. Ceram. Soc.* **59** (1976) 87.
15. A. G. EVANS and S. M. WIEDERHORN, *J. Mater. Sci.* **9** (1974) 270.
16. J. J. PETROVIC, L. A. JACOBSON, P. K. TALTY and A. K. VASUDEVAN, *J. Amer. Ceram. Soc.* **58** (1975) 113.
17. F. F. LANGE, *J. Amer. Ceram. Soc.* **56**, (1973) 518.
18. R. K. GOVILLA, Ford Motor Company Interim Report AMMRC TR 78-29, Contract DAAG-46-77-C-0028 (1978).
19. F. F. LANGE, Rockwell International Science Center Technical Report No. 4 (SC5117.4 TR) Contract N00014-77-C-0441 (1978).

Received 13 March and accepted 29 March 1979.